Liquid Polymorphism and Double Criticality in a Lattice Gas Model

Vera B. Henriques,[1,*] Nara Guisoni,[1,†] Marco Aurélio Barbosa,[1] Marcelo Thielo,[2] and Marcia C. Barbosa[2,‡]

[1] *Instituto de Física, Universidade de São Paulo, Caixa Postal 66318, 05315970, São Paulo, SP, Brazil*

[2] *Instituto de Física, UFRGS, 91501-970, Porto Alegre, RS, Brazil*

(Dated: April 1, 2005)

Abstract

We analyse the possible phase diagrams of a simple model for an associating liquid proposed previously. Our two-dimensional lattice model combines oreintational ice-like interactions and ¨Van der Waals¨ interactions which may be repulsive, and in this case represent a penalty for distortion of hydrogen bonds in the presence of extra molecules. These interactions can be interpreted in terms of two competing distances, but not necessarily soft-core. We present mean-field calculations and an exaustive simulation study for different parameters which represent relative strength of the bonding interaction to the energy penalty for its distortion. As this ratio decreases, a smooth disappearance of the double criticality occurs. Possible connections to liquid-liquid transitions of molecular liquids are suggested.

PACS numbers: 64.70.Ja, 05.70.Ce, 05.10.Ln

*Electronic address: vhenriques@if.usp.br

†Electronic address: nara@if.usp.br

‡Electronic address: barbosa@if.ufrgs.br

I. INTRODUCTION

The recently acknowledged possibility of the existence of single component systems which display coexistence between two different liquid phases [1][2] has opened many interesting questions regarding the link between the interaction potential and the presence of double criticality .

Network-forming fluids are primary candidates for liquid-liquid transitions. They exhibit directional, intermolecular attractions that lead to the formation of bonds between molecules. As a result, locally structured regions have lower density than unbonded regions. These structures at the fluid phase are transient and local but become permanent at lower temperatures.

The case of water is probably the network-forming liquid most intensively studied, due to its ubiquity in nature. An unstable liquid-liquid transition ending in a critical point was initially proposed to explain the anomalous behavior of network-forming liquids such as water [1][3]-[6]. Closely associated with the possibility of a liquid-liquid phase transition in supercooled water is the phenomenon of polyamorphism occurring below the glass transition temperature, T_g. Polyamorphism refers to the occurrence of distinct amorphous solid forms. There is by now a general consensus that water displays a transition between two different amorphous states in the supercooled region of its phase diagram [7]. Experiments carried out in water at $T \approx 130\ K$ show an abrupt change of volume as a function of pressure which indicates the existence of a first-order transition [8]. The two amorphous phases of water might be related to two different liquid phases at higher temperatures. At coexistence, these two liquid phases determine a first-order transition line ending at a critical point. Simulations and experiments predict that the liquid-liquid transition is in an experimentally inaccessible region of the phase-diagram [1][9][10][11].

Notwithstanding of its confirmation for metastable water, the coexistence of two liquid phases was uncovered as a possibility for a few both network-forming and non-bonding liquids. Computer simulations for realistic models for carbon [2], phosphorus [12], germanium [13], silica (SiO_2) [14][15] [16][17] and silicon [18][19] suggest the existence of a first-order transition between two liquid phases. Recent experiments for phosphorus [20][21] or phosphate compounds [22], and for carbon [23] confirm these predictions.

Substances that are structurally similar to water, such as Si, Ge, GeO_2 and silica, can

exhibit not only the liquid-liquid transition but also the other thermodynamic and dynamic anomalies present in water. Particular attention has been given to silica because its technological applications. Many intriguing properties of liquid silica and water occur at low temperatures. Examples include negative thermal expansion coefficients and polymorphism for both liquids. Compression experiments on silica show a non-trivial change in the microscopic structure [24][25]. This behavior, reproduced by simulations [26]-[28], was interpreted as an indication of a first-order transition. Inspired by these results, new simulations for different models for silica were performed [14][15] [16], giving support to the hypothesis of a first-order transition in silica. However, experiments must sill confirm a discontinuous transition between these amorphous phases [24][29].

In resume, a full understanding of the effects of the number, spatial orientation, and strength of bonds on the global fluid-phase behavior of network fluids is still lacking.

In order to gain some understanding, a number of simple models have been proposed. Since the work of Bernal [30], the water anomalies have been described in terms of the the presence of an extensive hydrogen bond network which persists in the fluid phase [31]. In the case of lattice models, the main strategy has been to associate the hydrogen bond disorder with bond [11][32] or site [33][34] Potts states. In the former case coexistence between two liquid phases may follow from the presence of an order-disorder transition and a density anomaly is introduced *ad hoc* by the addition to the free energy of a volume term proportional to a Potts order parameter. In the second case, it may arise from the competition between occupational and Potts variables introduced through a dependency of bond strength on local density states.

A different approach is to represent hydrogen bonds through ice variables[35][37][36][38], so successful in the description of ice [39] entropy, for dense systems. In this case, an order-disorder transition is absent. Recently a description based also on ice variables but which allows for a low density ordered structure [40] was proposed. Competition between the filling up of the lattice and the formation of an open four-bonded orientational structure is naturally introduced in terms of the ice bonding variables and no *ad hoc* introduction of density or bond strength variations is needed. Our approach bares some resemblance to that of some continuous models[41][42][43], which, however, lack entropy related to hydrogen distribution on bonds. Also, the reduction of phase-space imposed by the lattice allows construction of the full phase diagram from simulations, not always possible for continuous models [41]. In

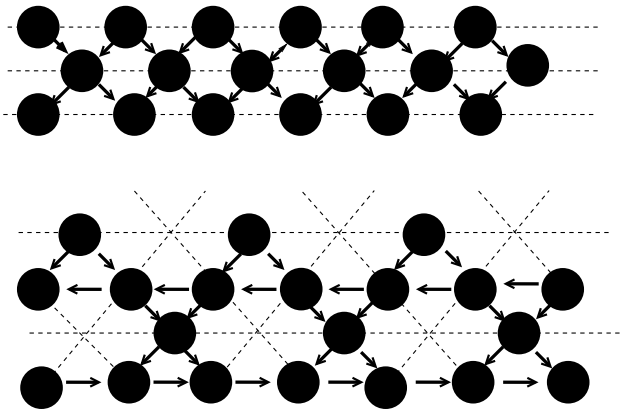

FIG. 1: High density liquid, HDL with density 1 (top) and low density liquid, LDL with density 3/4 (bottom)on the triangular lattice. The solid lines indicate the hydrogen bonds where the arrows differentiate bond donors from bond acceptors.

our previous publication, we have shown that this model is able to exhibit for a convenient set of parameters both density anomalies and the two liquid phases. Here we explore the phase space for various values of the orientational energy term. We show that by varying the relative strength of the orientational part, we can go at a fixed temperature from two coexisting liquid phases as observed in amorphous water to a smooth transition between two amorphous structures as might be the case of silica.

The remainder of the paper goes as follows. In sec. II the model is revised, for clarity. In sec. III mean-field results are given. Sec. IV has the simulations results. Conclusions end this session.

II. THE MODEL

Consider a lattice gas on a triangular lattice with sites which may be full or empty. Besides the occupational variables, σ_i, associated to each particle i, there are six other variables, τ_i^{ij}, pointing to neighboring sites j: four are the usual ice bonding arms, two donor, with $\tau_i^{ij} = 1$, and two acceptor, with $\tau_i^{ij} = -1$, while two additional opposite arms are taken as inert (non-bonding), $\tau_i^{ij} = 0$, as illustrated in Fig. 1. Therefore each occupied site is allowed to be in one of eighteen possible states.

Two kinds of interactions are considered: isotropic "van der Waals" and orientational hydrogen bonding. An energy $-v$ is attributed to each pair of occupied neighboring sites

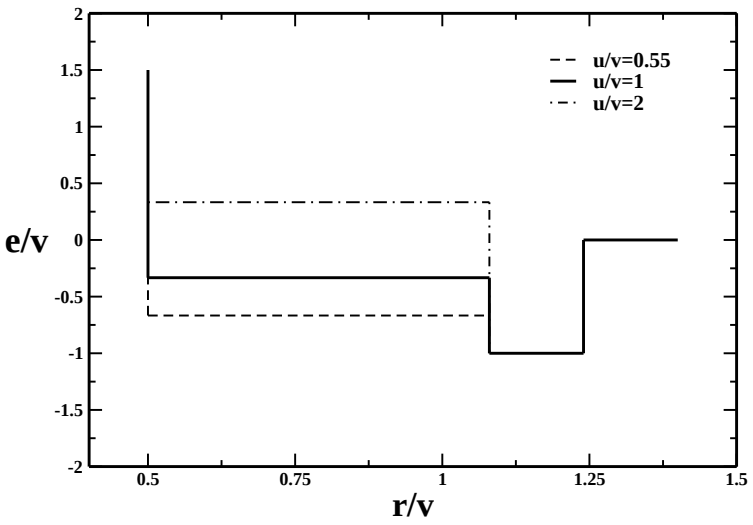

FIG. 2: Effective potential vs. inter-particle distance for u/v=1 (full-line), u/v=0.5 (dashed line) and u/v=2 (dot-dashed line). In the first case penalty on non-bonding neighbors is sufficient to stabilize de low density phase, whereas in the second case only the high density phase is stable at zero temperature. The step potential is accordingly "smoother". In the last case the shoulder becomes repulsive.

that form a hydrogen bond, while non-bonding pairs have an energy, $-v + 2u$ (for $u > 0$), which makes $-2u$ the energy of a hydrogen bond. The overall model energy is given by

$$E = \sum_{(i,j)} \{(-v + 2u)\sigma_i\sigma_j + u\sigma_i\sigma_j\tau_i^{ij}\tau_j^{ji}(1 - \tau_j^{ij}\tau_j^{ji})]\} \tag{1}$$

where $\sigma_i = 0, 1$ are occupation variables and $\tau_i^{ij} = 0, \pm 1$ represent the arm states described above. Note that each particle may have six neighbors, but the number of bonds per molecule is limited to four. For $u/v > 1/2$, the ¨van der Waals¨ forces become repulsive. As a result, each molecule attracts four neighbors, if properly oriented, and repeals the other two. An interpretation for this ¨repulsion¨ would be that the presence of the two extra neighbors distorts the electronic orbitals, thus weakening the hydrogen bonds.

Inspection of the model properties allows the prediction of two ordered states, as shown in Fig. 1. For low chemical potential, the soft core repulsion becomes dominant, $\rho = 0.75$, and energy ¨volume¨ density is given by $e = E/V = -3v/2$, where V is the number of lattice sites. If the chemical potential is high, $\rho = 1$, and energy density $e = -3v + 2u$. At zero temperature, the low density liquid (LDL) coexists with the high density liquid (HDL)

at chemical potential $\mu/v = -6 + 8u/v$, obtained by equating the grand potential density (or pressure) associated with each one of these phases. Similarly the coexistence pressure at zero temperature is given by $p/v = -3 + 6u/v$. Besides these two liquid states, a gas phase is also found and it coexists with the low density liquid at chemical potential $\mu/v = -2$ and pressure $p = 0$. The condition for the presence of the two liquid phases is therefore $u/v > 0.5$, i.e., that the "Van der Waals" interactions are repulsive.

The two ordered structures could be qualitatively associated to different ice phases. Under pressure, hydrogen bonds reorganize in more dense phases [44].

Our model may be interpreted in terms of some sort of average soft-core potential for large hydrogen bond energies. The low density phase implies average interparticle distance $\overline{d_{LD}} = \rho_{LD}^{-1/2} = 2/\sqrt{3}$, whereas for the high density phase we have $\overline{d_{HD}} = \rho_{HD}^{-1/2} = 1$. The corresponding energies per pair of particles is $-v$ and $-v+2u/3$. The hard core is offered by the lattice. For $u/v > 3/2$, the shoulder becomes repulsive, making the potential soft-core. Figure 2 illustrates, in a schematic way, the average pair energy e/v dependence on distance between particles, for $u/v = 1, 0.5, 2$. Notice that for $u/v = 2$ the potential at high density phases becomes repulsive. For $u/v = 1, 0.5$, the shoulder is attractive.

III. THE MEAN-FIELD ANALYSIS

Designing a correct mean-field version of the model is not an obvious task, due to the special orientational ice-like interactions. We have therefore looked at model properties on the Bethe lattice, for which exact relations may be given. Each site of the usual Cayley tree (of coordination six) is replaced by a hexagon and (η, τ) variables are attributed to its vertices (see Fig. 3), with η and τ defined as in the previous section. This representation is inspired on the Bethe solution for a generalization of the square water model [38, 46] presented by Izmailian et al. [45], [46]. For an occupied site-hexagon, we will have two vertices with $(\eta, \tau) = (1, 1)$, two with $(\eta, \tau) = (1, -1)$ and another two with $(\eta, \tau) = (1, 0)$. For an empty site-hexagon the six vertices have $(\eta, \tau) = (0, 0)$.

The partition function in the grand canonical ensemble is given by:

$$\Xi(T, \mu) = 18 e^{\beta\mu} g_N^2(1, +) g_N^2(1, -) g_N^2(1, 0) + g_N^6(0, 0), \tag{2}$$

where μ is the chemical potential and $g_N(1, +)$ is the partial partition function (generation

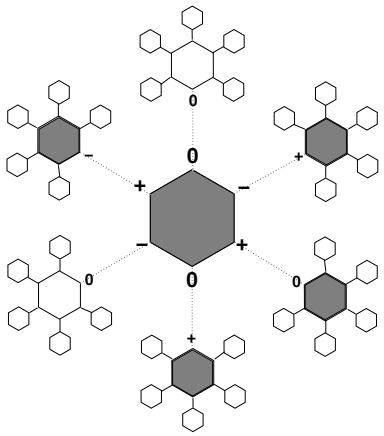

FIG. 3: The Bernal model on the Bethe lattice. Each site of an usual Bethe lattice is placed by a hexagon with (η, τ) variables placed on the vertices. Sites of the N generation are linked by dashed lines.

N) for a central site with $(\eta, \mu) = (1, 1)$. Similarly for $g_N(1, -)$, $g_N(1, 0)$ and $g_N(0, 0)$.

On each lattice line we have two (η, τ) pairs of variables connecting two consecutive generations of the lattice. The Boltzmann weights for each lattice line are $\omega = 1$, if at least one of the connecting sites is empty, and, if both sites are occupied, either $\omega = e^{\beta v}$, if arm variables are of opposite sign, and $\omega = e^{\beta(v-2u)}$, otherwise.

The density of water molecules at the central site of the tree is given by

$$\rho(T, \mu) = \frac{18z}{18z + x_N^2 y_N^2 r_N^2}, \tag{3}$$

where $z = e^{\beta\mu}$ is the activity and

$$x_N \equiv \frac{g_N(0,0)}{g_N(1,+)}, \qquad y_N \equiv \frac{g_N(0,0)}{g_N(1,-)}, \qquad r_N =\equiv \frac{g_N(0,0)}{g_N(1,0)}.$$

Eqn.3 gives us a relation between the water density ρ and the activity z: $6z = \gamma(x_N y_N r_N)^2$, with $\gamma = \rho/(3(1-\rho))$. Using this result the recursion relations at the fixed point may be written as

$$\begin{aligned} x &= \frac{\gamma(x+y+r)+1}{\gamma e^{\beta(v-2u)}(x+e^{2\beta u}y+r)+1}, \\ y &= \frac{\gamma(x+y+r)+1}{\gamma e^{\beta(v-2u)}(e^{2\beta u}x+y+r)+1}, \\ r &= \frac{\gamma(x+y+r)+1}{\gamma e^{\beta(v-2u)}(x+y+r)+1}. \end{aligned} \tag{4}$$

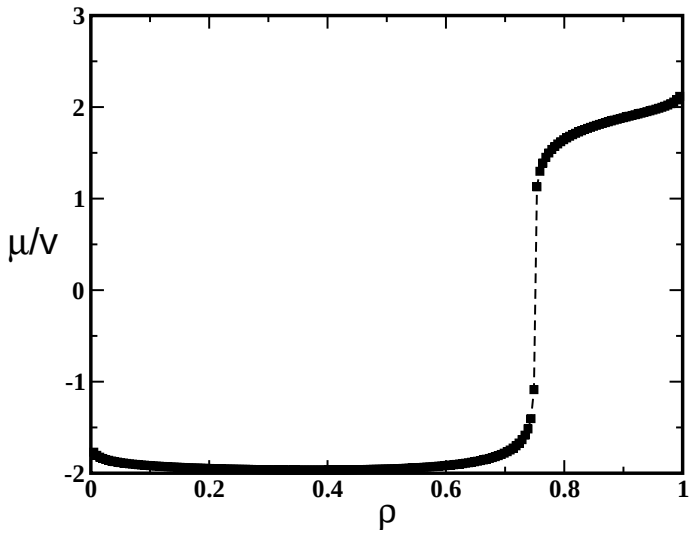

FIG. 4: Chemical potential versus water density for $u/v = 1$ and $\bar{T} = 0.05$. The coexistence between a gas ($\rho \sim 0$) and a low density phase ($\rho \sim 0.75$) can be seen from the van der Waals loop. Note the abrupt increase for $\rho \simeq 0.75$.

Under the the physical conditions $x \geq 0$, $y \geq 0$ and $r \geq 0$, since x, y and r are ratios between partition functions, we must have $x = y$. Eqs.4 reduce to two equations which are solved numerically for specific values of the model parameters u/v. Chemical potential vs density isotherms are then obtained from Eq.3, as shown in Figures 4 and 5.

The first striking result is that temperature destabilizes the liquid-liquid transition. Van der Waals loops are present only for the gas-liquid, but not for the liquid-liquid transition. However, for larger bond energies $u/v > 0.5$, the liquid phase is of low density ($\rho = 0.75$), whereas for smaller bond energies, the liquid phase is of high density ($\rho = 1$). A typical isotherm for the first case, for which the gas-liquid transition is to a phase of low density, is shown in Fig 4, for $u/v = 1$. It is to be noted that the chemical potential presents a very abrupt rise, just above the gas-liquid transition, as if signaling a quasi liquid-liquid transition. Fig 5 shows a typical low temperature isotherm for the second case, for $u/v = 0.25$, for which no low density phase is found.

Inspite of the absence of a liquid-liquid transition, present in the results of simulations (see [40] and next section), both the LD and the HD phases appear, for different strengths of the hydrogen bonds. Also, the abrupt rise of the chemical potential in Fig.4 indicates that the mean-field treatment comes near to but misses the LD-HD transition. A similar

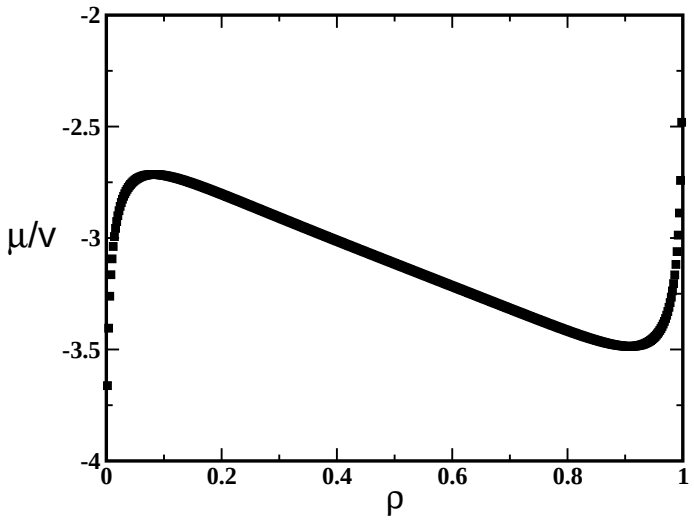

FIG. 5: Chemical potential versus water density for $u/v = 0.25$ for $\bar{T} = 0.4$. The LD phase is no longer present, since coexistence is between a gas ($\rho \sim 0$) and a high density phase ($\rho \sim 1$).

problem was noted by Izmailian et al [45] for the square model analyzed in their work. Cyclic ordering of edges around a vertex, in the lattice ordered structure, cannot be represented on the tree, which may lead to analytical free-energies for the same parameters for which exact [45] or simulation [40] studies predict phase transitions.

IV. THE MONTE CARLO RESULTS

The model properties for finite temperatures were obtained through Monte Carlo simulations in the grand-canonical ensemble using the Metropolis algorithm. Particle insertion and exclusion were tested with transition probabilities given by $w(insertion) = exp(-\Delta\phi)$ and $w(exclusion) = 1$ if $\Delta\phi > 0$ or $w(insertion) = 1$ and $w(exclusion) = exp(+\Delta\phi)$ if $\Delta\phi < 0$ with $\Delta\phi \equiv \exp\{\beta(e_{particle} - \mu) - \ln(18)\}$ where $e_{particle}$ is the particle energy. Since the empty and full sites are visited randomly, the factor 18 is required in order to guarantee detailed balance.

A detailed study of the model properties was presented in a previous publication for a particular value of the energy parameter, $u/v = 1$ [40]. Here, we present the evolution of the phase diagram under variation of this energy parameter which represents relative energy of bond strength. Note that the relevant parameter range is $u/v > 1/2$. For $u < v/2$, the LDL

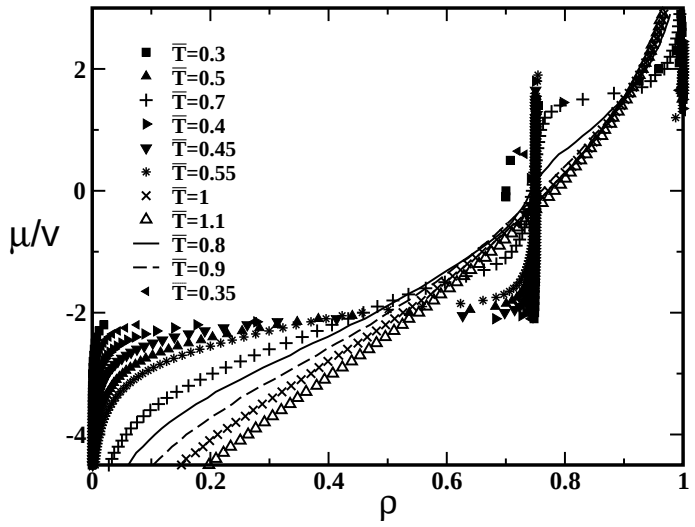

FIG. 6: Chemical potential vs. density isotherms for different temperatures. ρ is given in units of lattice space and the $\bar{T} = k_B T/v$. Here we illustrate the case $u/v = 1$.

disappears. Our study is for L=10 and runs were of the order of 10^6 Monte Carlo steps.

Chemical potential vs. density isotherms for different relative bond strengths parameters, $u/v = 1, 0.75, 0.6, 0.55$, and a large set of temperatures are illustrated in Fig.6. The figure shows the first-order phase transitions between the gas and the low density liquid phase and between the low density liquid and high density liquid phases. The coexistence lines are estimated from the mid-gaps in the chemical potentials. Fig. 7 illustrates the chemical potential vs. temperature phase-diagram for the same set of energy parameters. The gas-LDL coexistence lines for $u/v = 1, 0.75, 0.6, 0.55$ seem to collapse into a single line that at zero temperature gives $\mu/v = -2$. The different LDL-HDL lines are also illustrated. At zero temperature, exact calculations locate the end-points of these lines at, respectively, $\mu/v = 2, 0, -1.2, -1.6$. As $u/v \to 0.5$ the liquid-liquid coexistence lines approach the gas-liquid transition, merging with it at $u/v = 0.5$.

Pressure was computed from numerical integration of the Gibbs Duhem equation, at fixed temperature, from zero pressure at zero density. Fig. 8 shows the corresponding pressure vs temperature phase diagrams.

At zero temperature, we have the exact values $p/v = 3, 1.5, 0.6, 0.3$. An inversion of the LDL-HDL phase boundary, close to the critical point, is to be noted. The LDL-HDL line has positive slope for $u/v = 1, 0.75$, and negative slope for $u/v = 0.55$. This indicates that

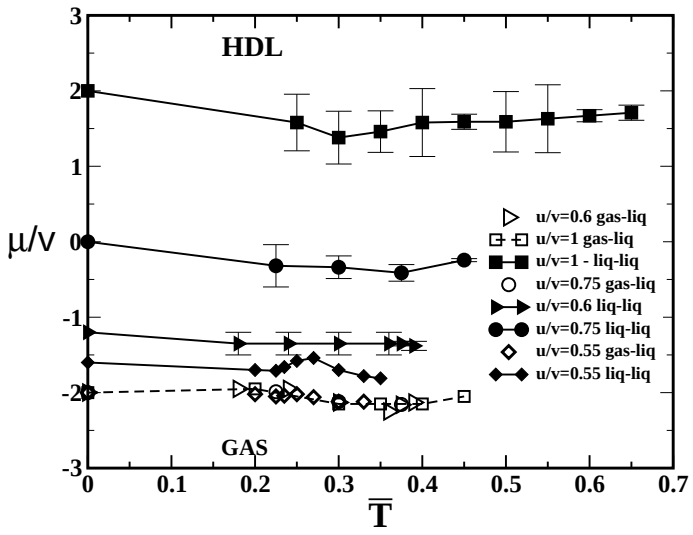

FIG. 7: Phase-diagram showing chemical potential vs. temperature for $u/v = 1, 0.75, 0.6, 0.55$. The solid lines are the LDL-HDL coexistence lines. The gas-LDL collapse into a single dashed line. The coexistence at zero temperature at $\mu/v = 2, 0, -1.2, -1.6$ and at $\mu/v = -2$ are exact. For visualization purposes the error bars for the gas-liquid points are not shown.

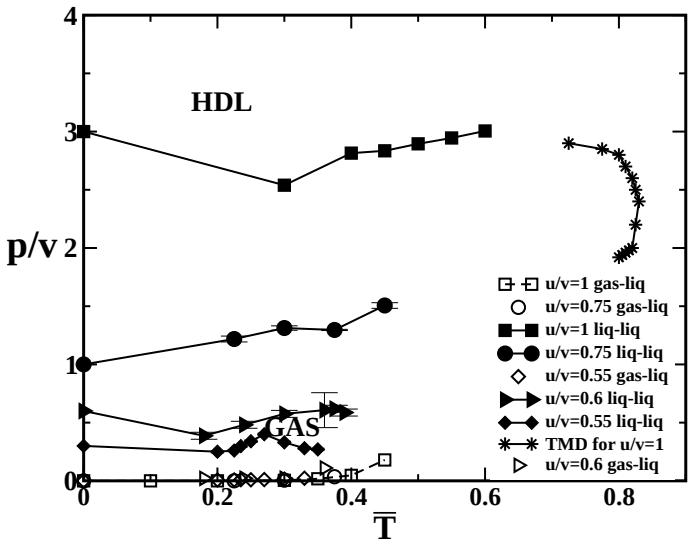

FIG. 8: Phase-diagram showing pressure vs. temperature for $u/v = 1, 0.75, 0.6, 0.55$. Reduced pressure p/v is given in units of lattice space. The solid lines (and filled symbols) are the LDL-HDL coexistence lines. The empty symbols indicate the gas-LDL coexistence lines collapsed into a single dashed line. The coexistence at zero temperature at $p/v = 3, 1.5, 0.6, 0.3$ and $p/v = 0$ are exact. For visualization purposes the error bars for the gas-liquid points are not shown.

for $u/v = 1, 0.75$ the low density liquid phase is more entropic than the high density liquid phase as it would be the case for most liquids. However, for $u/v = 0.55$, the LDL phase is less entropic than the HDL phase, a behavior that is expected for water. The line of temperature of maximum densities, TMD, is present for all $u/v > 0.5$ values. The figure illustrates the TMD only for the $u/v = 1$ case.

In summary, we have shown, both from mean-field and from simulatios that the model we proposed in a previous publication may present two liquid phases and the associated double criticality, depending on the ratio of bond strength to energy penalty for distortion, represented by our parameter u/v. Double criticality disappears in case the price paid for increasing the coordination is too high. A second consequence of varying the relative energies is that the slope of the liquid-liquid line may become negative, around the critical point.

Analysis of the model behaviour shows that the two liquids are present if the two competing distances are sufficiently separated, but the ¨shoulder¨ need not be negative (see Fig. 2), in contradiction to a recent proposal [47]. In other words, two caracteristic attractive distances might also generate the liquid-liquid transition.

Experimental and numerical evidence suggests that water possesses a first-order transition between a low density liquid and a high density liquid. The present model shows two liquid phases and consequently two critical points and a line of density anomalies.

Experimental evidence for a first-order transition in silica is still missing. According to our model, as the bond energy varies, the critical point temperature decreases. For temperatures above the critical point, under compression the liquid goes from the low density phase to high density phase in a continuous way as it is observed experimentally in silica. Since the liquid-liquid critical point moves to lower temperatures as the bond energy becomes weaker, one could suggest that the first-order transition predicted by simulations is not observed in experiments because the coexistence line and the second critical point in the case of silica might be located at very low temperatures.

Water and silica are network bonding systems, and present low-coordination solids with transition to higher coordinated solids at high pressures. Ice I is tetrahedrally bonded, with bonds suffering distortion, for higher pressures. At still higher pressures, the tetrahedral structures interpenetrate, to satisfy both energy and pressure requirements. Silica transitions between tetrahedrally and octahedrally coordinated structures. It would be interesting to establish energy criteria for bond distortions in both cases, in order to test the ideas we

propose in this study.

Acknowledgments

This work was supported by the Brazilian science agencies CNPq, FINEP, Fapesp and Fapergs.

---

[1] P.H. Poole, F. Sciortino, U. Essmann, and H. E. Stanley, Nature **360**, 324 (1992); Phys. Rev. E **48**, 3799 (1993); F. Sciortino, P.H. Poole, U. Essmann, and H.E. Stanley, Ibid **55**, 727 (1997); S. Harrington, R. Zhang, P.H. Poole, F. Sciortino, and H.E. Stanley, Phys. Rev. Lett. **78**, 2409 (1997).

[2] J. N. Glsli and F. H. Ree, Phys. Rev. Lett. 82, 4659 (1999).

[3] P. G. Debenedetti, Metastable Liquid: Concepts and Principles, Princeton University Press, Princeton, 1998.

[4] M. -C. Bellisent-Funel, e., Hydration Processes in Biology: Theoretical and Experimental Approaches, NATO ASI Series A, Vol 305, IOS Press, Amsterdam, 1998.

[5] G. W. Robinson, S. Singh, S. -B. Zhu and M. W. Evans, Water in Biology, Chemistry and Physics , World Scientific , Singapore, 1996.

[6] C. A. Angell and R. J. Rao, J. Chem. Phys. 57, 470 (1972).

[7] O. Mishima and H. E. Stanley, Nature 396, 329 (1998).

[8] O. Mishima, L. D. Calvert and E. Whalley, Nature 310, 393 (1984); O. Mishima, K. Takemura and K. Aoki, Science 254, 406 (1991); O. Mishima, J. Chem. Phys. 100, 5910 (1994).

[9] H. Tanaka, J. Chem. Phys. 105, 5099 (1996); Nature 380, 328 (1996).

[10] O. Mishima, Phys. Rev. Lett. 85, 334 (2000); Mishima and Y. Suzuki, Nature (London) 419, 599 (2002).

[11] G. Franzese, M.I. Marques and H.E. Stanley, Phys Rev E 67, 011103 (2003).

[12] T. Morishita, Phys. Rev. Lett. 87, 105701 (2001).

[13] M. Durandurdu and D.A. Drabold, Phys. Re. B 66, 041201 (2002)

[14] P. H. Poole, M. Hemmati and C. A. Angell, Phys. Rev. Lett. 79, 2281 (1997).

[15] I. Saika-Voivod, F. Sciortino and P. H. Poole, Phys. Rev. E 63, 011202 (2001); I. Saika-Voivod, P. H. Poole and F. Sciortino, Nature 412, 514 (2001).

[16] D.J. Lacks, Phys. Rev. Lett. 84, 4629 (2000)

[17] L.P. Huang, L. Duffrene and J. Kieffer, J. Non-Cryst. Sol. 349, 1 (2004)

[18] C. A. Angell, S. Borick and M. Grabow, J. Non-Cryst. Solids 207, 463 (1996); see also M. Kaczmarski, O.N. Bedoya-Martinez and E.R. Hernandez, Phys. Rev. Lett. 94, 095701 (2005)

[19] C.E. Miranda and A. Antonelli, J. Chem. Phys. 120, 11672 (2004)

[20] Y. Katayama, T. Mizutani, W. Utsumi, O. Shimomura, M. Yamakata and K. Funakoshi, Nature 403, 170 (2000).

[21] G. Monaco, S. Falconi, W.A. Crichton and M. Mezouar, Phys. Rev. Lett. 90, 255701 (2003).

[22] R. Kurita and M. Tanaka, Science 306, 845 (2004)

[23] M. Togaya, Phys. Rev. Lett 79, 2474 (1997).

[24] M. Grimsditch, Phys. Rev. Lett. 52, 2379 (1984).

[25] R. J. Hemley, H. K. Mao, P. M. Bell and B. O. Mysen, Phys. Rev. Lett. 57, 747 (1986).

[26] M. S. Samyazulu et. al, J. Phys: Condens. Matter 5, 6345 (1993).

[27] J. S. Tse, D. D. Klug and Y. Lepage, Phys. Rev. B 46, 5933 (1992).

[28] W. Jin, R. K. Kalia, P. Vshishta and J. P. Rino, Phys. Rev. Lett. 71, 3146 (1993).

[29] Q. Williams and R. Jeanloz, Science 239, 902 (1988).

[30] J.D. Bernal and R.H. Fowler, J. Chem. Phys. 1, 515 (1933).

[31] Tests of the cooperativity of the net are still being tested, e.g. J.R. Errington, P.G. Debenedetti and S. Torquato, Phys. Rev. Lett. 89, 215503 (2002).

[32] S. Sastry, P. G. Debenedetti, F. Sciortino and H.E. Stanley, Phys Rev E 53, 6144 (1996).

[33] S. Sastry, F. Sciortino and H. E. Stanley, J. Chem. Phys. 98, 9863 (1993)

[34] C.J. Roberts and P.G. Debenedetti, J Chem Phys 105, 658 (1996)

[35] C.-K. Hu, J. Phys. A:Math.Gen.16 L321 (1983);

[36] P. Attard, Physica A233, 742 (1996)

[37] W. Nadler and T. Krausche Phys. Rev. A 44, R7888 (1991)

[38] N. Guisoni and V.B. Henriques, Braz. J. Phys. 30, 736 (2000).

[39] E.H. Lieb, Phys. Rev. Lett. 18, 692 (1967).

[40] V. B. Henriques and M. C. Barbosa, "Liquid Polymorphism and Density Anomaly in a Lattice Gas Model", Phys. Rev. E (to be published).

[41] K.A.T. Silverstein, A.D.J.Haymet and K.A. Dill, J. Am. Chem. Soc. 120, 3166 (1998).

[42] T.M.Truskett, P.G. Debenedetti, S. Sastry and S. Torquato, J. Chem. Phys. 111, 2647 (1999).

[43] T.M.Truskett and K.A. Dill, J. Chem. Phys. 117, 5101 (2002).

[44] D. Eisenberg and W. Kauzmann, *The Structure and Properties of Water*, Clarendon Press 1969.

[45] N. Sh. Izmailian, C.-K. Hu and F.Y. Wu, J. Phys. A: Math. Gen. 33, 2185 (2000).

[46] N. Guisoni and V. B. Henriques, *Square water as a simplified solvent model*, in preparation.

[47] G. Franzese, G. Malescio, A. Skibinsky, S. Buldyrev and E.H. Stanley, Nature, 409, 682 (2001).